Dipole-quadrupole interference spectroscopy: Observation of an autoionizing He ^1D Rydberg series

B. Krässig, E. P. Kanter, S. H. Southworth, and L. Young
Argonne National Laboratory, Argonne, Illinois 60439, USA

R. Wehlitz
Synchrotron Radiation Center, University of Wisconsin, Stoughton, Wisconsin 53589, USA

B. A. deHarak
Department of Physics and Astronomy, University of Kentucky, Lexington, Kentucky 40506-0055, USA and Physics Department, Illinois Wesleyan University, Bloomington, Illinois 61702-2900, USA

N. L. S. Martin
Department of Physics and Astronomy, University of Kentucky, Lexington, Kentucky 40506-0055, USA
(Received 23 March 2012; revised manuscript received 9 October 2012; published 12 November 2012)

We have used dipole-quadrupole interference spectroscopy to observe an optically forbidden quadrupole Rydberg series of helium autoionizing levels. The technique measures the forward-backward asymmetry of photoelectron angular distributions produced in the vacuum ultraviolet photoionization of helium. The resonant behavior of this asymmetry in the region of a quadrupole autoionizing level enables the determination of the position, width, and Fano line-profile parameter q of the level. We have obtained these quantities for the He $_2(1,0)_n^+$ ^1D Rydberg series for $n = 2$–7. We find that for $n \geqslant 3$ all three quantities have the expected n scaling, with a quantum defect of 0.31. For $n \geqslant 3$ the average q parameter lies close to zero, whereas for $n = 2$ it is negative.

DOI: 10.1103/PhysRevA.86.053408 PACS number(s): 32.80.Zb, 32.30.Jc

I. INTRODUCTION

One of the most important and versatile tuneable sources for atomic spectroscopy is synchrotron radiation, first proposed as a spectroscopic tool in the 1940s and developed during the 1950s [1,2]. An important milestone in the use of synchrotron radiation, and of particular interest here, was the first observation of doubly excited He autoionizing levels by Madden and Codling in 1963 [3]. They detected the first eight members of the main Rydberg series with orbital momentum $L = 1$, of which the lowest may be designated He $2s2p(^1P)$ and higher members as mixtures of $2snp$ and $2pns$ [4].

The arrival of far-ultraviolet synchrotron radiation sources allowed the systematic exploration of autoionizing levels of many atoms. Helium was investigated with increasingly high resolution, culminating in the benchmark experiments of Domke *et al.* [5], who clearly resolved the main He autoionizing ^1P series up to $n = 16$, in addition to many other extremely weak series. The strong electron-electron correlation effects present in He preclude a single-configuration description and the $(sp,2n\pm)$ scheme (originally called the $(2n\pm)$ scheme [4]) may be used for two of the optically allowed series while the $_N(K,T)_n^A$ classification scheme [6] (also written as $_n(K,T)_N^A$ [7–10]) may be used for both optically allowed and optically forbidden series. The quantities K and T correspond to angular, and A radial, correlations of the two electrons in a hyperspherical coordinate description of He. A discussion of these schemes is given in Ref. [10], for example.

A limitation of absorption spectroscopy is that only certain types of energy levels can be observed. Levels excited by a dipole transition can readily be seen, but those excited by a quadrupole transition cannot because the absorption cross section is reduced by a factor of $\alpha^2 < 10^{-4}$, where $\alpha \approx 1/137$ is the fine-structure constant [11]. Thus, since He has a ^1S ground state, ^1P, but not ^1D, autoionizing states are observed in absorption experiments using synchrotron radiation.

In fact, it is possible to observe ^1D autoionizing states *indirectly* by isolating the quantum-mechanical dipole-quadrupole interference term that occurs in the angular distribution of the emitted photoelectrons. This cross term is of order α compared with the dipole cross section and hence may be seen as an $\sim 1\%$ effect. In recent years there have been dipole-quadrupole interference studies of individual autoionizing levels in Cd [11] and He [12,13].

The helium experiment [12,13] demonstrated that it was possible to obtain ^1D autoionizing level positions, widths, and Fano q parameters [14] from the interference term. We have named this technique dipole-quadrupole interference spectroscopy (DiQuIS). An important aspect of the technique is the ability to obtain the true value of the ^1D q parameter. As noted in our previous work [12,13], this cannot be obtained from charged-particle scattering experiments because the substantial presence of octupole and higher multipoles affects the observed line profile. In photoionization the quadrupole-octupole interference term is a factor of α^2 smaller than the quadrupole-dipole interference term and may be ignored. Here we present DiQuIS measurements of the He $_2(1,0)_n^+$ ^1D Rydberg series [8]; this series may also be approximately described as $2pnp$ ^1D.

II. THEORY

The dipole-quadrupole interference term has been quantified in the asymmetry parameter γ which appears in the

photoelectron angular distribution appropriate to helium [15],

$$\frac{d\sigma(\theta,\phi)}{d\Omega} = \frac{\sigma_1}{4\pi}(3\cos^2\theta + \gamma \sin\theta\cos^2\theta\cos\phi). \quad (1)$$

Here σ_1 is the dipole photoabsorption cross section, the radiation is incident in the x direction and linearly polarized along the z axis, and the photoelectron direction is given in spherical polar coordinates. For reflection through the origin the interference term changes sign but the dipole term does not. Thus the difference between measurements at different directions can be used to extract γ.

In the absence of autoionization σ_1 and γ are slowly varying functions of energy. However, Eq. (1) is also valid when autoionization is present. For the $L = 1,2$ Rydberg series of autoionizing levels with energy E_{nL} of interest here, all members have linewidths Γ_{nL} much less than level separations $|E_{nL} - E_{(n\pm1)L}|$. Equation (1) may therefore be applied to each individual pair of dipole and quadrupole levels of the same n, with the substitution of the resonant forms of the dipole cross section σ_{n1}^R and dipole-quadrupole interference parameter γ_n^R. These are given by [12]

$$\sigma_{n1}^R = \sigma_1 \frac{(q_{n1} + \varepsilon_{n1})^2}{1 + \varepsilon_{n1}^2} \quad (2)$$

and

$$\gamma_n^R = \gamma_0 \left\{ \frac{\cos(\delta_2 - \delta_1 + \Delta_{n2} - \Delta_{n1})}{\cos(\delta_2 - \delta_1)} \right\} \times \left\{ \frac{q_{n2} + \varepsilon_{n2}}{(1 + \varepsilon_{n2}^2)^{1/2}} \right\} \Big/ \left\{ \frac{q_{n1} + \varepsilon_{n1}}{(1 + \varepsilon_{n1}^2)^{1/2}} \right\}. \quad (3)$$

For each resonance q_{nL} is the Fano line profile index and $\varepsilon_{nL} = (\omega - E_{nL})/(\Gamma_{nL}/2)$ is the energy with respect to the resonance position measured in units of the half-width of the resonance. The phase of each unperturbed continuum wave is δ_L and the extra phase shift due to autoionization Δ_{nL} is given by $\cot\Delta_{nL} = -\varepsilon_{nL}$ [14].

The values of the dipole cross section $\sigma_1(E_n)$, the asymmetry parameter $\gamma_0(E_n)$, and the continuum phases $\delta_L(E_n)$ are those that would exist in the absence of any resonances and are all assumed to be constant in the region $E_n = (E_{n1} + E_{n2})/2$ of each pair of resonances. On the other hand, σ_{n1}^R and γ_n^R vary rapidly in the region of a pair of resonances. Thus the experimental behavior of γ_n^R yields the positions, widths, and Fano q parameters of quadrupole resonances.

III. EXPERIMENT

The experiments were carried out on the plane-grating monochromator beamline at the Synchrotron Radiation Center, University of Wisconsin–Madison using an electron spectrometer system designed and built at Argonne National Laboratory. The electron spectrometer uses four parallel-plate electron analyzers mounted on a rotation stage at the magic angle with respect to the rotation axis and with the rotation axis perpendicular to the photon beam direction and polarization axis. The asymmetry parameter γ is determined from differences of photoelectron intensities measured at selected angles of the rotation axis. Details are given in Refs. [13,16].

The construction of γ involves two quantities, the *sum* and *difference* spectra, for each n, which are separately used to extract the parameters of the quadrupole resonances. The sum spectra give high-quality photoabsorption cross sections σ_{n1}^R, which when fitted to Eq. (2) yield the experimental energy resolution and the E_{n1}, Γ_{n1}, and q_{n1} for each n. For the

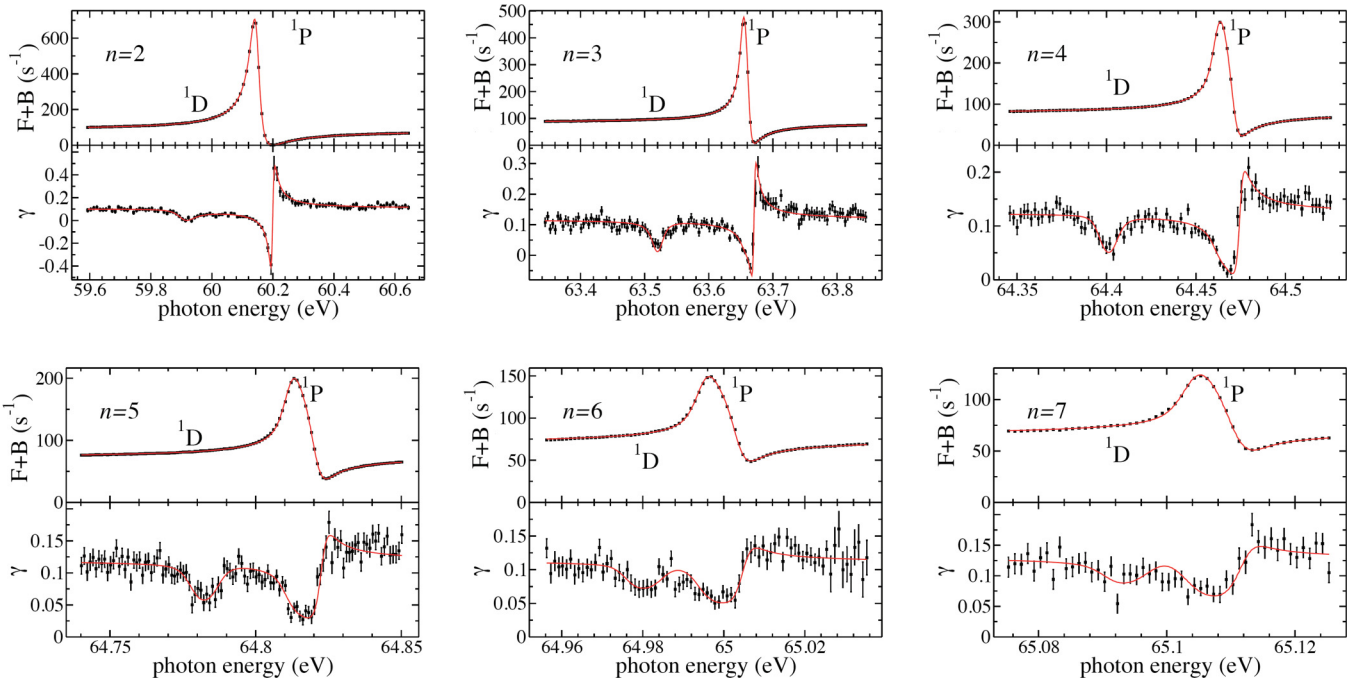

FIG. 1. (Color online) Energy dependence of the dipole cross section σ_{n1} for He $(sp,2n+)$ ^1P (top of each panel; see the text) and asymmetry parameter γ for He $_2(1,0)_n^+$ ^1D and $(sp,2n+)$ ^1P (bottom of each panel) autoionizing Rydberg series for n = 2–7. The data and statistical errors are indicated in each figure as discrete points. The fits, described in the text, are shown as solid lines.

present experiments the resolution depends on the setting of the monochromator slits and the full width at half maximum of the Gaussian instrument function is approximately 11 meV for $n = 2$, 8 meV for $n = 3$–6, and 7 meV for $n = 7$. These parameters are then used in a fit of the difference spectra, which are proportional to the product $\sigma_{n1}^R \gamma_n^R$ given by Eqs. (2) and (3). (Note that the use of this form eliminates problems encountered with singularities—even though folded with the energy resolution—when trying to fit γ directly [17].) The fits yielded the quadrupole resonance parameters E_{n2}, Γ_{n2}, and q_{n2}; the $\gamma_0(E_n)$; and the relative phases $\delta_2(E_n) - \delta_1(E_n)$.

We also investigated the use of instrument functions that differ from a pure single Gaussian function. In particular, a function consisting of two, slightly separated, identical Gaussian functions give slightly better fits to the dipole cross section in the region of the minima for $n = 5$–7 for which the resonance widths are significantly narrower than the instrument function. However, the fitted parameters are no different (to within the fitting uncertainties) from the single Gaussian instrument function. The results given in this paper therefore use a pure single Gaussian instrument function for all n.

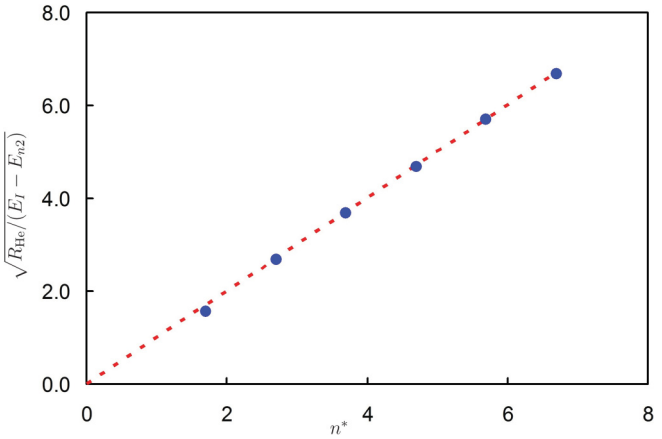

FIG. 2. (Color online) Plot of the experimental resonance energies in the form $\sqrt{R_{\rm He}/(E_I - E_{n2})}$ vs n^* for quantum defect $\mu_{n2} = 0.31$. (The error bars are smaller than the size of the symbols.) The straight line is Eq. (5).

IV. RESULTS AND DISCUSSION

The experimental data for $n = 2$–7 and their fits are shown in Fig. 1. The top part of each panel shows the dipole cross section formed from the sum of the count rates of the forward (F) and backward (B) photoelectron detector signals. The bottom part of each panel shows the experimental asymmetry parameter γ, formed from differences and sums in the photoelectron detectors. The fitted curves for γ are obtained by dividing the fitted curves to the difference spectra by the fitted sum spectra. All the fitted curves shown correspond to reduced χ^2 values close to unity.

Table I presents the corresponding values of the fitted parameters, where they are compared with those from our earlier experiment on $n = 2$ [12], ejected-electron spectroscopy [18,19], ion-impact data [20], and theoretical calculations [6,18]. Our energy scales are calibrated using the known positions of ^1P resonances [3,10]; this introduces an extra uncertainty in E_{n2} of 4 meV [10] in addition to the fitting uncertainties shown in the table. In general, the agreement with the values found from the various experimental techniques and theory is very good.

TABLE I. Energies E_{n2}, widths Γ_{n2}, and q_{n2} parameters of He $_2(1,0)_n^+$ ^1D $n = 2$–7 autoionizing levels. The experimental values (this work) are the result of fitting Eq. (3) to the data of Fig. 1. Other workers' experimental values are from Refs. [12,18–20]. The theoretical values of energies and widths (and their range in parentheses) are a compilation of those in Refs. [6,18] and references therein. The numbers in parentheses for the experimental data are uncertainties in the last digits: 0.0649(65) means 0.0649 ± 0.0065.

	This work			Experiment			Theory	
n	E_{n2} (eV)	Γ_{n2} (eV)	q_{n2}	E_{n2} (eV)	Γ_{n2} (eV)	q_{n2}	E_{n2} (eV)	Γ_{n2} (eV)
2	59.911(4)	0.0649(65)	−0.19(10)	59.905(5)[a] 59.903(8)[b] 59.89(3)[c] 59.85(9)[d]	0.057(3)[a] 0.052(21)[b] 0.072(18)[c]	−0.25(7)[a]	59.950(45)	0.0676(34)
3	63.522(2)	0.0178(22)	0.12(16)	63.515(9)[b] 63.50(3)[c] 63.51(4)[d]	0.012(8)[b]		63.529(13)	0.0161(10)
4	64.401(1)	0.0056(6)	−0.04(14)	64.400(8)[b] 64.39(3)[c] 64.44(2)[d]			64.408(8)	0.0068(5)
5	64.782(1)	0.0040(5)	0.22(19)	64.804(23)[b]			64.789(9)	0.0034(2)
6	64.984(1)	0.0026(4)	0.15(27)				64.988(9)	0.0021(3)
7	65.098(2)	0.0015(6)	0.39(72)				65.096(1)	0.0012(0)

[a]Reference [12].
[b]Reference [18].
[c]Reference [19].
[d]Reference [20].

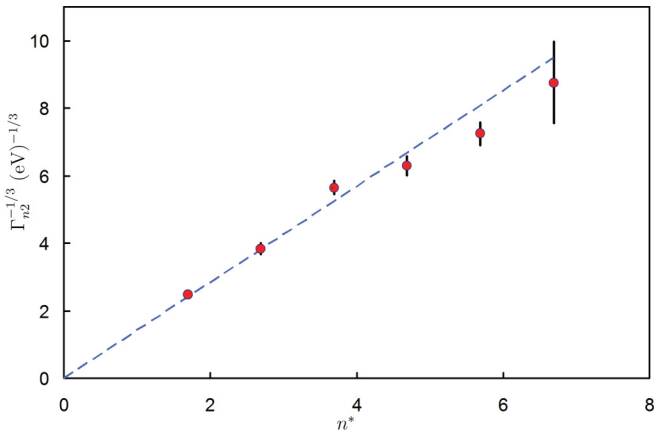

FIG. 3. (Color online) Plot of the experimental resonance widths in the form $\Gamma_{n2}^{-1/3}$ vs n^* for quantum defect $\mu_{n2} = 0.31$. The straight line is a least-squares fit that passes through the origin.

The results of our present experiment are consistent with those of the earlier experiment on $n = 2$ [12]; the slightly smaller fitted uncertainties of the latter reflect its longer run times and hence better statistics. Note also that the poorer energy resolution of the earlier experiment (≈20 meV) results in a much weaker observed modulation of γ (Ref. [12], Fig. 1) in the region of the narrow (37 meV) $n = 2$ ^1P resonance than that of the present experiment, whereas the much broader ^1D resonance is relatively unaffected.

For well-behaved Rydberg series of autoionizing levels, the energies, widths, and Fano q parameters should obey certain relationships [14,21]. The energies above the ground-state neutral atom should be given by

$$E_I - E_{n2} = \frac{R_{\rm He}}{(n-\mu_{n2})^2} = \frac{R_{\rm He}}{(n^*)^2}, \tag{4}$$

where E_I is the ionization potential that leaves the He^+ ion in the $N = 2$ state, $R_{\rm He} = 13.6038$ eV is the Rydberg constant for neutral helium [10], μ_{n2} is the quantum defect of the quadrupole series, and $n^* = n - \mu_{n2}$ is the effective quantum number. This may be rearranged as

$$\sqrt{\frac{R_{\rm He}}{E_I - E_{n2}}} = n^*. \tag{5}$$

This relationship is tested in Fig. 2 for our experimental data, which, for $n \geqslant 3$, are in good agreement with Eq. (5) with $\mu_{n2} = 0.31$. (The data point for $n = 2$ lies slightly away from the straight line, as expected for the lowest member of a Rydberg series.)

This agreement implies that the widths Γ_{n2} should be approximately proportional to $(1/n^*)^3$, which follows from the fact that the inner part of the wave functions for each n differ only by a normalization factor [21]. Although this is strictly valid only for $n \gg 1$, our results are in quite good agreement with this approximation, as can be seen in Fig. 3, which plots $\Gamma_{n2}^{-1/3}$ vs n^* and where the straight line is a linear least-squares fit constrained to pass through the origin.

Finally, the Fano line profile index q_{n2} should be independent of n since it is given by the ratio of two matrix elements that have the same n scaling [21]. Figure 4 shows that our experimental values are consistent with a weighted average of $q_{n2} = -0.04 \pm 0.06$. For $n = 2$, a value of $q_{22} = -0.19 \pm 0.10$ is only just compatible with this average and is

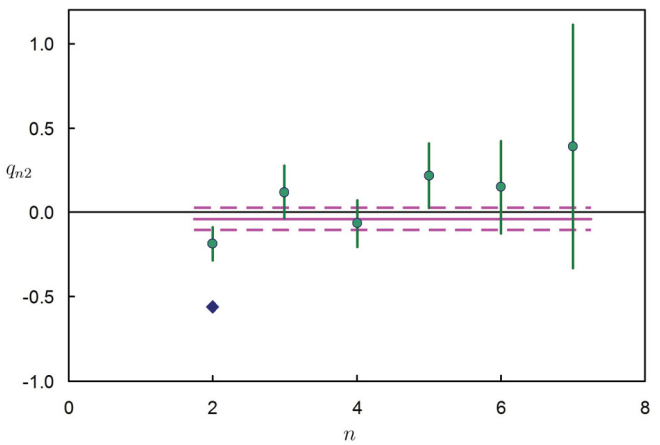

FIG. 4. (Color online) Circles, the experimental Fano line profile parameters q_{n2} vs n. Diamond, the first-order electron-impact calculation from Ref. [22] (see the text). The horizontal solid and dashed lines are the weighted average and uncertainty of the experimental q_{n2}, respectively.

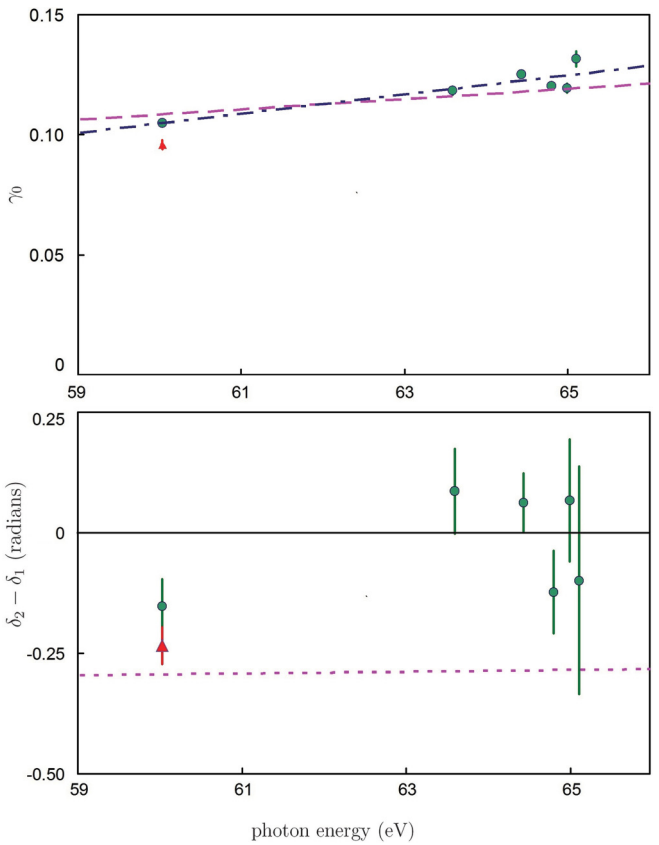

FIG. 5. (Color online) Top: circles, experimental γ_0 vs photon energy; triangle, value from Ref. [12]. Except where shown, the uncertainties are less than the size of the symbols. The dashed line is the RPAE calculation from Ref. [13]. The dash-dotted line is a linear fit to the data. Bottom: circles, experimental unperturbed phase differences $\delta_2 - \delta_1$ vs photon energy; triangle, value from Ref. [12]. The dotted line is the RPAE calculation from Ref. [13].

in fact significantly more negative than any of the other q_{n2}. We note that ${}_2(1,0)_n^+ \, {}^1D$ for $n = 2$ may be represented by an almost pure $2p^2$ configuration, whereas for $n \geqslant 3$ the nominal $2pnp$ configurations may contain an admixture of $2snd$. It is possible that even a small admixture may profoundly affect the excitation mechanism (e.g., via $1s \rightarrow nd$ accompanied by $\langle 1s|2s\rangle$ overlap). Also shown in the figure is a calculation of q_{22} for high-incident-energy electron-impact ionization using the R matrix with pseudostates (RMPS) approach [22]. At high incident energies a first-order calculation asymptotically approaches that for photoionization [23]. RMPS photoionization calculations are called for to compare the $n = 2$ with the $n \geqslant 3$ q parameters.

The fits also yield values of the nonresonant γ_0 and $\delta_2 - \delta_1$ in the energy region of each pair of resonances. These are plotted in Fig. 5, where they are compared with the random-phase approximation with exchange (RPAE) calculations from Ref. [13]. The calculated γ_0 is in quite good agreement with the experimental results. Also shown in the top panel is a linear fit to the data; although there is some scatter to the data, all points lie within 2.5σ of the line, where σ is their fitted uncertainty. The calculated $\delta_2 - \delta_1$ in the bottom panel is not in good agreement with the fitted data. Although the latter have large uncertainties, they suggest that the phase difference lies close to zero for $n > 2$.

V. CONCLUSION

We have used DiQuIS to measure the energies, widths, and Fano asymmetry parameters of a Rydberg series of autoionizing levels in helium excited from the ground state by a quadrupole transition. Although these levels can be observed using charged-particle-impact ionization [18], the excitation mechanisms are fundamentally different. Particle impact involves many multipoles and a pure quadrupole q parameter cannot be extracted; it has also been shown that such a q parameter is a complex quantity with equally important real and imaginary parts [22]. There are also postcollision interaction effects which distort the line shape and shift the resonance position. Finally, the energy resolution of a particle-impact experiment [18] is typically an order of magnitude worse than that of a synchrotron experiment, which severely curtails the maximum observable n of a Rydberg series.

Our results highlight the need for theoretical calculations of the quadrupole series q parameters and new calculations of γ_0 and $\delta_2 - \delta_1$ over the energy range covered by our experiments.

ACKNOWLEDGMENTS

This work was supported by the Chemical Sciences, Geosciences, and Biosciences Division of the Office of Basic Energy Sciences, Office of Science, US Department of Energy, under Contract No. DE-AC02-06CH11357. N.L.S.M. acknowledges support from National Science Foundation Grant No. PHY-0855040. We are grateful for the help and hospitality of the staff of the Synchrotron Radiation Center (SRC). The University of Wisconsin SRC was supported by National Science Foundation Grant No. DMR-0537588.

[1] E. M. Rowe and F. E. Mills, Part. Accel. **4**, 211 (1973).
[2] D. H. Tomboulian and P. L. Hartman, Phys. Rev. **102**, 1423 (1956).
[3] R. P. Madden and K. Codling, Phys. Rev. Lett. **10**, 516 (1963).
[4] J. W. Cooper, U. Fano, and F. Prats, Phys. Rev. Lett. **10**, 518 (1963).
[5] M. Domke, C. Xue, A. Puschmann, T. Mandel, E. Hudson, D. A. Shirley, G. Kaindl, C. H. Greene, H. R. Sadeghpour, and H. Petersen, Phys. Rev. Lett. **66**, 1306 (1991).
[6] M.-K. Chen, Phys. Rev. A **56**, 4537 (1997).
[7] D. R. Herrick and O. Sinanoglu, Phys. Rev. A **11**, 97 (1975).
[8] C. D. Lin, Phys. Rev. A **29**, 1019 (1984).
[9] C. D. Lin, Adv. At. Mol. Phys. **22**, 77 (1986).
[10] M. Domke, K. Schulz, G. Remmers, G. Kaindl, and D. Wintgen, Phys. Rev. A **53**, 1424 (1996).
[11] N. L. S. Martin, D. B. Thompson, R. P. Bauman, C. D. Caldwell, M. O. Krause, S. P. Frigo, and M. Wilson, Phys. Rev. Lett. **81**, 1199 (1998).
[12] B. Krässig, E. P. Kanter, S. H. Southworth, R. Guillemin, O. Hemmers, D. W. Lindle, R. Wehlitz, and N. L. S. Martin, Phys. Rev. Lett. **88**, 203002 (2002).
[13] E. P. Kanter, B. Krässig, S. H. Southworth, R. Guillemin, O. Hemmers, D. W. Lindle, R. Wehlitz, M. Y. Amusia, L. V. Chernysheva, and N. L. S. Martin, Phys. Rev. A **68**, 012714 (2003).
[14] U. Fano, Phys. Rev. **124**, 1866 (1961).
[15] J. W. Cooper, Phys. Rev. A **47**, 1841 (1993).
[16] B. Krässig, J.-C. Bilheux, R. W. Dunford, D. S. Gemmell, S. Hasegawa, E. P. Kanter, S. H. Southworth, L. Young, L. A. LaJohn, and R. H. Pratt, Phys. Rev. A **67**, 022707 (2003).
[17] L. Argenti and R. Moccia, J. Phys. B **43**, 235006 (2010).
[18] B. A. deHarak, J. G. Childers, and N. L. S. Martin, Phys. Rev. A **74**, 032714 (2006).
[19] P. J. Hicks and J. Comer, J. Phys. B **8**, 1866 (1975).
[20] K. Iemura, S. Ohtani, H. Suzuki, J. Takeda, S. Machida, K. Tanabe, T. Takayanagi, K. Wakiya, M. Sekiguchi, Y. Kanai, S. Kitazawa, X. M. Tong, S. Sakaguchi, T. Watanabe, and F. J. Currell, Phys. Rev. A **64**, 062709 (2001).
[21] U. Fano and J. W. Cooper, Phys. Rev. **137**, 1364 (1965).
[22] N. L. S. Martin, B. A. deHarak, and K. Bartschat, J. Phys. B **42**, 225201 (2009).
[23] B. A. deHarak, J. G. Childers, and N. L. S. Martin, J. Electron Spectrosc. Relat. Phenom. **141**, 75 (2004).